Numerical Study of Supersonic Molecular Beam Injection System in Thailand Tokamak I*)

Jiraporn PROMPING, Apiwat WISITSORASAK[1,2], Boonyarit CHATTHONG[3,4] and Kewalee NILGUMHANG

Thailand Institute of Nuclear Technology (Public Organization), Nakhon Nayok, Thailand
[1)]*Theoretical and Computational Physics Group, Department of Physics, Faculty of Science, King Mongkut's University of Technology Thonburi, Bangkok, Thailand*
[2)]*Center of Excellence in Theoretical and Computational Science, Faculty of Science, King Mongkut's University of Technology Thonburi, Bangkok, Thailand*
[3)]*Department of Physics, Faculty of Science, Prince of Songkla University, Songkhla, Thailand*
[4)]*CompAnIS-BSC Research Center, Faculty of Science, Prince of Songkla University, Hat Yai, Thailand*

(Received 29 November 2019 / Accepted 2 April 2020)

Thailand Institute of Nuclear Technology (TINT) is planning to develop Thailand Tokamak I from HT-6 M tokamak. In the first phase of operation, the device will be equipped with two fueling systems: gas puffing (GP) and supersonic molecular beam injection (SMBI). Since the SMBI system has never been used experimentally with this device, this work, therefore, numerically studies the penetration features of SMBI in the plasma of Thailand Tokamak I, based on the nominal parameters of HT-6 M tokamak. The interaction of the supersonic molecules with the plasma has been computed by BOUT++ code which solves six-field fluid model of SMBI model in the radial direction. The preliminary results demonstrate that the SMBI is an efficient method for fueling the plasma and the beam can be delivered to the center of the plasma core.

Keywords: tokamak, fueling system, SMBI, BOUT++

DOI: 10.1585/pfr.15.2403033

1. Introduction

Thailand Institute of Nuclear Technology (TINT) is developing Thailand Tokamak I from a former tokamak HT-6 M in the collaboration with Institute of Plasma Physics, Chinese Academy of Science (ASIPP) [1, 2]. The device will be located in the main campus of TINT in Nakhon-Nayok province in Thailand. Several components of the tokamak such as auxiliary heating systems, optical diagnostic, data acquisition systems, will be upgraded and installed. For the fueling systems, the device will employ the gas puff (GP) [3, 4], and the supersonic molecular beam injection (SMBI) [5]. Note that the pellet injection (PI) system which can effectively deliver the fuel to tokamaks [6–8] may be used in the future. Since the role of the molecular gas at the edge of tokamaks has very complex nature and involves with many atomic phenomena. The SMBI technique has also never been used with this tokamak. The aim of this research is therefore to investigate the feasibility of SMBI system on the plasma of TT1 based on the nominal parameters of HT-6 M, see Table 1, by using a simulation which is based on a fluid model.

The supersonic molecular beam injection is considered as one of the best schemes for fueling the plasma [9]. It is also experimentally and computationally demonstrated to be more efficient than the GP method since the fuels can be delivered deeper into the plasma [10]. In addition, the SMBI yields comparable penetration depth of the deposited fuel as fueling scheme using the injection of pellets. Nowadays the SMBI have been widely applied to many tokamak devices such as HL-2A [11], KSTAR [12], W7-AS [13], JT-60U [14], and EAST [15]. Furthermore, the construction cost of the SMBI system is less than that of the PI system. Therefore, it may be considered more attractive than the PI system, especially for a small tokamak such as TT1.

Previously, Wang *et. al.* used TPSMBI code to simulate the transport of the molecular beam to HL-2A toka-

Table 1 Plasma parameters of TT1.

Parameters	Physical Descriptions	Values
R (m)	Major radius	0.65
a (m)	Minor radius	0.20
I_p (kA)	Plasma current	100
B_T (T)	Toroidal field on axis	1.5
κ	Elongation	1.0
δ	Triangularity	1.0

author's e-mail: apiwat.wis@kmutt.ac.th
*) This article is based on the presentation at the 28th International Toki Conference on Plasma and Fusion Research (ITC28).

mak [16]. The results showed that the density peak of the fueling particles was appeared at $r/a = 0.8$ and the temperatures in the fueling region [16]. However, the penetration depth of the injection beam also depends several factors such as the size of a tokamak, the injection direction and speed, and the properties of the background plasma [17]. In this work, we attempt to computationally investigate the effect of the injection speed of the molecular beam and the density of the background plasma on the penetration depth of the fueling beam in TT1 tokamak. The interaction of the molecular beam and the plasma has been carried out by using the 1D SMBI model and numerically solve within the framework of BOUT++code [18].

This paper is organized as follows. We first describe the transport models, and relevant transport equations and parameters in section 2. In the section 3we present the numerical results for two cases: 3.1) the sensitivity of the injection speed and 3.2) the impact of the injection in the low and high plasma densities. Finally, section 4 summarizes the present work.

2. Physical Model and Numerical Method

The supersonic molecular beam injection delivers the fueling gas, such as hydrogen or deuterium, into a tokamak from the edge. Once these molecules reach the hot background plasma, they undergo many collisions and are subjected to complex plasma phenomenasuch as atomic dissociation, charge exchange, and ionization. In this work, we simplify the fueling model [16, 17] with only dominant atomic processes. Here four kinds of particle species are considered in this model: hydrogen molecules, hydrogen atoms, ions, and electrons. By assuming the poloidal and toroidal symmetries, a set of the transport equations is reduced to one dimension in the radial direction. The schematic picture of the beam injection along the radial direction is illustrated in Fig. 1.

For the background plasma, we assume the quasi-neutrality condition. The radial transport equations of the

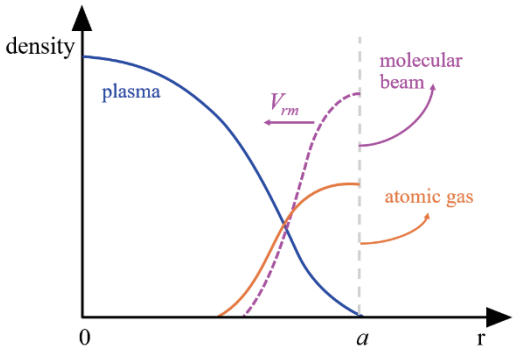

Fig. 1 The transport of the molecular beam along the radial direction. The beam travels with speed V_{rm} into the plasma, and subsequently dissociates into atomic gas.

electron density (n_e), the electron temperature (T_e) and the ion temperature (T_i) can be written as follows [16]:

$$\frac{\partial n_e}{\partial t} - D_{\perp e}\left(\frac{1}{r}\frac{\partial n_e}{\partial r} + \frac{\partial^2 n_e}{\partial r^2}\right) = S_I^p, \tag{1}$$

$$\frac{\partial T_e}{\partial t} - \frac{2}{3}\chi_{\perp e}\left(\frac{1}{r}\frac{\partial T_e}{\partial r} + \frac{\partial^2 T_e}{\partial r^2}\right) = -v_I\left(T_e + \frac{2}{3}W_I\right) - \frac{2}{3}v_{diss}W_{diss} - \frac{2m_e}{M_i}\frac{T_e - T_i}{\tau_e}, \tag{2}$$

$$\frac{\partial T_i}{\partial t} - \frac{2}{3}\chi_{\perp i}\left(\frac{1}{r}\frac{\partial T_i}{\partial r} + \frac{\partial^2 T_i}{\partial r^2}\right) = -v_I T_i - \frac{2m_e}{M_i}\frac{T_e - T_i}{\tau_e}, \tag{3}$$

where $D_{\perp e}, \chi_{\perp e}, \chi_{\perp i}$ are the radial diffusion coefficients of the electron density, the electron and ion temperatures, respectively. The particle source due to the atomic ionization (S_I^p) is defined as

$$S_I^p = n_e v_I = n_a v_I^a, \tag{4}$$

W_I and W_{diss} are the energy lost due to the ionization and dissociation processes and are approximately equal to $W_I = 20$ eV, and $W_{diss} = 4.5$ eV. The atomic ionization rate (v_I), and molecular dissociation rate (v_{diss}) are

$$v_I = n_a\langle\sigma_I V_{th,e}\rangle, v_{CX} = n_a\langle\sigma_{CX}V_{th,i}\rangle, \tag{5}$$

$$v_{diss} = n_e\langle\sigma_{diss}V_{th,e}\rangle. \tag{6}$$

Note that the energy exchange between electrons and ions is approximately calculated by the term $\frac{2m_e}{M_i}\left(\frac{T_e - T_i}{\tau_e}\right)$.

The transport equation of the molecular beam (n_m) is dominated by the convective transport due to the injection in the radial direction. It can be expressed as

$$\frac{\partial n_m}{\partial t} + \frac{1}{r}\frac{\partial}{\partial r}(rV_{rm}n_m) = -S_{diss}^p, \tag{7}$$

$$\frac{\partial V_{rm}}{\partial t} + V_{rm}\frac{\partial V_{rm}}{\partial r} = -\frac{1}{n_m M_m}\frac{\partial p_m}{\partial r}, \tag{8}$$

where $V_{\rm rm}$ is the radial velocity of the beam, S_{diss}^p is the particle sink due to the molecular dissociation, $P_m = k_B n_m T_m$ and is the molecular pressure. Here we simply assume that the temperature of the molecule is constant at the room temperature of 300 K. After the dissociation, the molecules separate into atoms and the transport of these atoms can be written as

$$\frac{\partial n_a}{\partial t} - D_{\perp a}\left(\frac{1}{r}\frac{\partial n_a}{\partial r} + \frac{\partial^2 n_a}{\partial r^2}\right) = S_I^p + 2S_{diss}^p, \tag{9}$$

where $D_{\perp a}$ is the radial diffusion coefficient of atoms. The atom source due to dissociation (S_{diss}^p) is computed by

$$S_{diss}^p = n_e v_{diss} = n_m v_{diss}^m, \tag{10}$$

where the dissociation rate $\nu^m_{diss} = n_m\langle\sigma_{diss}V_{th,e}\rangle$ and $\nu_{diss} = n_e\langle\sigma_{diss}V_{th,e}\rangle$. Note that the rate coefficients are empirically given by [16]

$$\langle\sigma_I V_{th,e}\rangle = 3\times10^{-8}\frac{(0.1T_e\,\mathrm{eV})^2}{[3+(0.1T_e\,\mathrm{eV})^2]}\,\mathrm{cm}^3/\mathrm{s}, \quad (11)$$

$$\langle\sigma_{CX}V_{th,i}\rangle = 1.7\times10^{-8} + 1.9\times10^{-8} \times\frac{(1.5T_i\,\mathrm{eV})^{1/3}-(15\,\mathrm{eV})^{1/3}}{(150T_i\,\mathrm{eV}^{1/3}-(15\,\mathrm{eV})^{1/3})}\,\mathrm{cm}^3/\mathrm{s}, \quad (12)$$

$$\langle\sigma_{diss}V_{th,e}\rangle = 3\times10^{-8}\frac{(0.1T_e\,\mathrm{eV})^2}{[3+(0.1T_e\,\mathrm{eV})^2]}\,\mathrm{cm}^3/\mathrm{s}. \quad (13)$$

The boundary conditions for n_e, T_i, and T_e are chosen to match with our previous simulations [19]:

$$\left.\frac{\partial n_e}{\partial x}\right|_{\mathrm{core}} = 10.52\times10^{20}\,\frac{\mathrm{m}^{-3}}{\mathrm{m}},$$
$$n_e|_{\mathrm{edge}} = 10^{18}\,\mathrm{m}^{-3},$$
$$\left.\frac{\partial T_{e,i}}{\partial x}\right|_{\mathrm{core}} = 499.2\,\frac{\mathrm{eV}}{\mathrm{m}},$$
$$T_{i,e}|_{\mathrm{core}} = 10\,\mathrm{eV}.$$

For the density of atomic:

$$\left.\frac{\partial n_a}{\partial x}\right|_{\mathrm{core}} = \left.\frac{\partial n_a}{\partial x}\right|_{\mathrm{edge}} = 0.$$

For the density of the injected molecules:

$$\left.\frac{\partial n_m}{\partial x}\right|_{\mathrm{core}} = 0, \quad n_m|_{\mathrm{edge}} = 10^{19}\,\mathrm{m}^{-3}.$$

For the radial velocity of the molecular beam:

$$\left.\frac{\partial V_{rm}}{\partial x}\right|_{\mathrm{core}} = 0, \quad V_{rm}|_{\mathrm{edge}} = -900\,\mathrm{m/s}.$$

The transport equations are numerically solved by numerical techniques implemented in BOUT++. It is worth noting that the convection term is treat by the WENO3 scheme [20] and the forth order central difference is applied to the first and second derivatives [18].

3. Simulation Results and Discussions

In this section, we simulate the plasma fueling by the supersonic molecular beam injection in Thailand Tokamak I by using the numerical scheme detailed in the previous section. We note that TTI is a small machine whose major and minor radii are 0.65 m and 0.20 m, respectively. The device employs a poloidal limiter for limiting the plasma and the shape of the plasma is nearly circular. In the initial phase of the operation, the hydrogen plasma will be used, and its average density will be in the range of 10^{18} - 10^{20} m^{-3}. The supersonic molecular beam of hydrogen gas will be delivered to the tokamak plasma from the low-field side (LFS) with variable injection speed. For simplicity, we also assume that amount of other impurities is negligible and are not considered in this work. The following subsections report the numerical results of the SMBI as the injection speeds and the densities of the background plasma are varied.

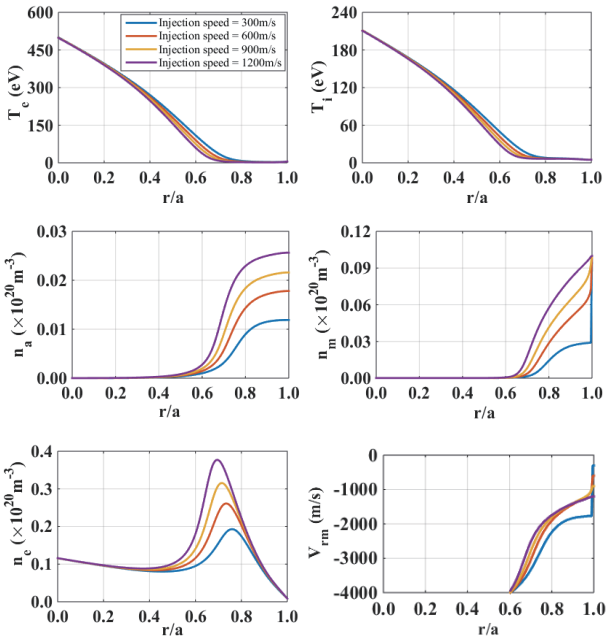

Fig. 2 The graphs show the radial profiles of the electron temperature (T_e), the ion temperature (T_i), the hydrogen atoms (n_a), the molecular density (n_m), the electron density (n_e), the molecular radial velocity (V_{rm}) at time of 100 µs after the injection with molecular radial velocity of 300 - 1200 m/s.

3.1 Sensitivity study of the injection speed

Injection speed of the beam is one of the critical quantities which subsequently determines the penetration depth and the fueling efficiency. This section studies the effect of the SMBI on the tokamak plasma at different injection speeds. Here the line average density of the hydrogen plasma of 6.3×10^{18} m^{-3} is assumed before the injection. When the SMBI system is triggered, the beam of the hydrogen molecules are launched into the plasma with the injection speed.

Figure 2 shows the radial profiles of the electron temperature (T_e), the ion temperature (T_i), the hydrogen atoms (n_a), the molecular density (n_m), the electron density (n_e), the radial velocity of the injected molecules (V_{rm}) at t = 100 µs after the beam of the supersonic molecule is injected at the different injection speeds. When the beam of the hydrogen gas reaches the edge of the plasma, it dissociates into hydrogen atoms and results in the increase of the density of the hydrogen atoms (n_a), see Fig. 3. Then the atoms are ionized and finally become part of the background plasma. We note that the radial speed of the molecular beam is strongly driven by the pressure gradient. At the edge, the speed is equal to the injection speed of the beam. It then rapidly increases at the propagating front of the molecular beam where the density of the molecular particles significantly decreases due to the dissociation of the molecules. Such decreasing density of the molecules also leads to the decrease of the molecular pressure (P_m).

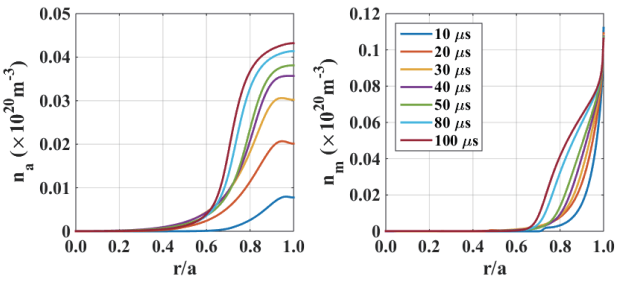

Fig. 3 The evolution of the density profile of the atomic gas and the injected molecules at different times. Note that the injection speed is 900 m/s.

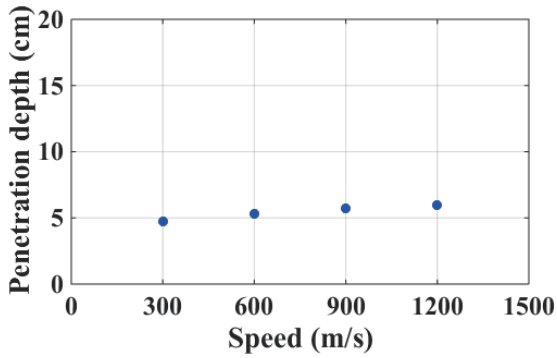

Fig. 4 The penetration depth as a function of the injection speed.

In the inner core ($r/a < 0.6$), the molecular density is zero. Thus, the radial speed keeps the value at the lower edge of the density front. Furthermore, we can see that the electron and ion densities have peaks near the edge at the normalized radius around 0.7 to 0.8. These graphs also show that the electron density peak is shifted towards the center as the injection speed increases.

In order to compare the impact of the injection speed on the penetration depth of the injected fuels, we define the penetration depth as the distance from the edge of the plasma density peak which was taken 100 μs after the injection. Figure 4 plots the penetration depth versus the injection speeds. This graph clearly shows that the faster injection speed yields the deeper penetration depth.

3.2 Comparison of the beam injections in the plasma with low and high densities

This section compares the effect of the SMBI after the beam was launched with constants speed of 300 m/s into the plasma with low plasma density ($\bar{n}_e = 6.3 \times 10^{18}$ m^{-3}) and high plasma density ($\bar{n}_e = 1.4 \times 10^{19}$ m^{-3}). When the SMBI is applied to the low-density case, it causes the density peak around the normalized radius about 0.7, see Fig. 5. However, the density peak is shifted radially outward for the plasma with higher density. This clearly suggests that faster injection speed is required for the higher density plasma for deeper deposition.

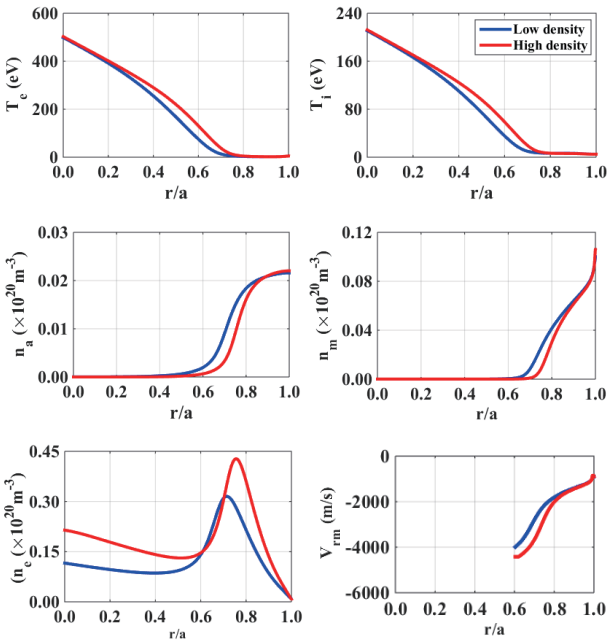

Fig. 5 The graphs show the radial profiles of the electron temperature (T_e), the ion temperature (T_i), the hydrogen atoms (n_a), the molecular density (n_m), the electron density (n_e), the molecular radial velocity (v_{rm}) as the beams are injected with speed of 900 m/s. Two cases of the background plasma density is compared: low density $n_e = 6.3 \times 10^{18}$ m^{-3}, and high density $n_e = 1.4 \times 10^{19}$ m^{-3}. These plots were taken at $t = 100$ μs after the SMBI is triggered.

4. Conclusion

In this work, we numerically study the SMBI in TT1 using a 6-field fluid model. The transport equations are numerically solved by the finite difference method from BOUT++ code. The model is simply treated by a slab geometry and the hydrogen plasma is assumed. The simulation shows that as the molecular beam of hydrogen is launched from the low-field side, the density of the hydrogen molecule increase. The atomic density is then increased due to the dissociation process. Consequently, the electron density rises due to the ionization, and the ion and electron temperatures continually drop. The density peak at the edge then slowly diffuses to the core. The faster injection speed yields the deeper penetration depth. It is found that, if we require the penetration depth about 6 cm, the minimum injection speed of 600 m/s to the plasma with average density of 10^{19} m^{-3} is required. However, the faster injection speed must be used if the tokamak is operated with higher plasma density.

Acknowledgment

This work was partly supported by the International Atomic Energy Agency (IAEA) under Contract No. 22785 and Thailand Research Fund (contract No. MRG6180175). The work is part of a collaborative re-

search project under the Center for Plasma and Nuclear Fusion Technology (CPaF). Computational facilities at Theoretical and Computational Physics Group, King Mongkut's University of Technology Thonburi is greatly appreciated.

[1] HT-6M Team, Fusion Technol. **9**, 476 (1986).
[2] J. Promping, S. Sangaroon, A. Wisitsorasak *et al.*, Plasma Fusion Res. **13**, 3403094 (2018).
[3] S. Sajjad, X. Gao, B. Ling *et al.*, Phys. Lett. A **373**, 1133 (2009).
[4] S.J. Zweben, D.P. Stotler, R.E. Bell *et al.*, Plasma Phys. Control. Fusion **56**, 095010 (2014).
[5] D.L. Yu, C.Y. Chen, L.H. Yao *et al.*, Nucl. Fusion **50**, 035009 (2010).
[6] L.R. Baylor, Nucl. Fusion **32**, 2177 (1992).
[7] W.A. Houlberg, S.E. Attenberger, L.R. Baylor *et al.*, Nucl. Fusion **32**, 1951 (1992).
[8] L.R. Baylor, T.C. Jernigan, C.J. Lasnier *et al.*, J. Nucl. Mater. **266-269**, 457 (1999).
[9] L. Yao, N. Tang, Z. Cui *et al.*, Nucl. Fusion **38**, 631 (1998).
[10] Z.H. Wang, X.Q. Xu, T.Y. Xia *et al.*, Nucl. Fusion **54**, 043019 (2014).
[11] S. Hong-Juan, D. Xuan-Tong, Y. Liang-Hua *et al.*, Plasma Phys. Control. Fusion **52**, 045003 (2010).
[12] W.W. Xiao, P.H. Diamond, W.C. Kim *et al.*, Nucl. Fusion **54**, 023003 (2014).
[13] Y. Lianghua and J. Baldzuhn, Plasma Sci. Technol. **5**, 1933 (2003).
[14] H. Takenaga, J. Nucl. Mater. **390-391**, 869 (2009).
[15] X. Zheng, J. Li, J. Hu *et al.*, Plasma Phys. Control. Fusion **55**, 115010 (2013).
[16] Y.-H. Wang, W.-F. Guo, Z.-H. Wang *et al.*, Chinese Phys. B **25**, 106601 (2016).
[17] Y.-L. Zhou, Z.-H. Wang, M. Xu *et al.*, Chinese Phys. B **25**, 095201 (2016).
[18] B.D. Dudson, M.V. Umansky, X.Q. Xu *et al.*, Comput. Phys. Commun. **180**, 1467 (2009).
[19] J. Promping, A. Wisitsorasak, B. Chatthong *et al.*, Plasma Fusion Res. **14**, 3403154 (2019).
[20] G.-S. Jiang and C.-W. Shu, J. Comput. Phys. **126**, 202 (1996).